Am J Transl Res 2021;13(8):8965-8976
www.ajtr.org /ISSN:1943-8141/AJTR0131810

Original Article

Superimposition of metabolic syndrome magnifies post-stenotic kidney injury in dyslipidemic pigs

Turun Song[1,2], Yu Zhao[1], Xiangyang Zhu[1], Alfonso Eirin[1], James D Krier[1], Hui Tang[1], Kyra L Jordan[1], Amir Lerman[3], Lilach O Lerman[1]

[1]Division of Nephrology and Hypertension, Mayo Clinic, Rochester, MN 55905, The United States; [2]Urology Department, Urology Research Institute, Organ Transplantation Center, West China Hospital, Sichuan University, Sichuan, China; [3]Department of Cardiovascular Diseases, Mayo Clinic, Rochester, MN 55905, The United States

Received February 11, 2021; Accepted May 12, 2021; Epub August 15, 2021; Published August 30, 2021

Abstract: Background: Dyslipidemia aggravates kidney injury distal to atherosclerotic renal artery stenosis (ARAS). Besides dyslipidemia, metabolic syndrome (MetS) also involves development of obesity and insulin-resistance (IR). We hypothesized that concurrent obesity and IR magnify swine stenotic-kidney damage beyond dyslipidemia. Methods: Pigs with unilateral RAS were studied after 16 weeks of atherogenic diets without (ARAS) or with (MetS + RAS) development of obesity/IR (n=6 each). Additional pigs on normal diet served as normal or non-dyslipidemic RAS controls (n=6 each). Stenotic-kidney renal blood flow (RBF), glomerular filtration rate (GFR), and microvascular architecture were studied using CT, and oxygenation was studied using blood oxygen level-dependent magnetic-resonance-imaging. We further compared kidney adiposity, oxidative stress, inflammation, apoptosis, fibrosis, and systemic levels of oxidative and inflammatory cytokines. Results: ARAS and MetS + RAS developed hypertension and dyslipidemia, and MetS + RAS also developed obesity and IR. RBF and GFR were similarly decreased in all post-stenotic pig kidneys compared to normal pig kidneys, yet MetS + RAS aggravated and expanded medullary hypoxia and microvascular loss. RAS and ARAS increased systemic levels of tumor necrosis factor (TNF)-α, which were further elevated in MetS + RAS. Renal oxidative stress and TNF-α expression increased in ARAS and further in MetS + RAS, which also upregulated expression of anti-angiogenic angiostatin, and magnified apoptosis, tubular injury, and fibrosis. Conclusion: Beyond dyslipidemia, obesity and insulin-resistance aggravate damage in the post-stenotic kidney in MetS, despite relative hyperfiltration-related preservation of renal function. These observations underscore the need to control systemic metabolic disturbances in order to curb renal damage in subjects with ischemic kidney disease.

Keywords: Renal artery stenosis, atherosclerosis, metabolic syndrome, dyslipidemia, insulin resistance

Introduction

Renal artery stenosis (RAS) is a major cause of secondary hypertension, and may result in renal and cardiac insufficiency [1]. Kidney impairment due to chronic hypoperfusion and ischemic nephropathy [2] imposes oxidative stress, inflammation, and fibrosis in the stenotic kidney, as well as loss of kidney function. In older individuals, atherosclerotic RAS (ARAS) is the most common etiology [3], which, in some individuals, might be complicated by concurrent metabolic disorders, including obesity, insulin resistance (IR), and hyperlipidemia [4].

Metabolic syndrome (MetS) is a cluster of metabolic abnormalities that are closely associated with increased cardiovascular, stroke, and all-cause mortality [5]. MetS is defined by the presence of three of five traits: abdominal obesity, high blood pressure, laboratory abnormalities of triglyceride, and high-density lipoprotein-cholesterol (HDL-C) levels, or IR [6]. MetS is present in approximately 20% of adults in the USA, and up to 50% of severely obese youngsters [7]. MetS has also been recognized as a risk factor for kidney injury with increased incidence of microalbuminuria or proteinuria [8], and ultimately increased risk for end-stage renal disease [9]. Of importance, each component of MetS is independently associated with increased risk for chronic kidney disease (CKD), and their coexistence magnifies its incidence [10].

We have shown that hyperlipidemia, a surrogate for early atherosclerosis, exacerbated stenotic kidney injury in ARAS [11]. Yet, in addition to hyperlipidemia [11, 12], development of IR and obesity during progression of MetS further aggravates cardiac injury [13], mitochondrial dysfunction, and fibrosis [14]. However, whether MetS deteriorates stenotic kidney injury beyond hyperlipidemia alone remains unknown. We hypothesized that superimposition of MetS, characterized by development of obesity and IR, would magnify ischemic kidney injury in pigs compared to dyslipidemia alone. Thus, we studied both in-vivo and ex-vivo stenotic kidneys from dyslipidemic pigs, with and without IR and obesity that characterize MetS. Dyslipidemia and MetS were achieved by feeding pigs with selective high-fat diets without or with additional high-carbohydrate components, respectively.

Materials and methods

The Institutional Animal Care and Use Committee of Mayo Clinic approved this study (A00003694-18). Three months-old domestic female pigs obtained from the same vendor (Manthei Hog Farm, Elk River, MN) were randomized into four groups (n=6 each). For 16 weeks, two groups (normal and RAS controls) were fed regular pig chow. To induce dyslipidemia, ARAS pigs consumed an atherogenic diet of 2% cholesterol and 15% lard (TD-93296, Harlan-Teklad), a surrogate of early atherosclerosis [11]. To induce dyslipidemia as well as obesity and IR, MetS + RAS pigs were fed a MetS-inducing diet (5B4L; Purina Test Diet, Richmond, Indiana) that contains (in % kcal) 17% protein, 20% complex carbohydrates, 20% fructose, and 43% fat supplemented with 2% cholesterol and 0.7% sodium cholate by weight [15].

In RAS, ARAS, and MetS + RAS pigs, a unilateral renal arterial obstruction was induced 6 weeks after diet initiation, to reproduce the clinical situation in which diffuse metabolic aberrations precede vascular obstruction. For this purpose, animals were anesthetized with telazol (5 mg/kg IM) and xylazine (2 mg/kg IM), and sedation was maintained with isoflurane (1.5%). A local-irritant coil was then placed in the right renal artery, as described previously [16]. A sham procedure was performed in one group of normal diet-fed animals, which were subsequently used as controls.

Four weeks later, under anesthesia, the degree of stenosis was determined by angiography, and fasting blood samples were collected from the inferior vena cava and stenotic renal vein for plasma renin activity (PRA), serum creatinine (both kits were from DiaSorin, Stillwater, MN, USA), and cytokine levels. All pigs were studied using blood oxygen level-dependent (BOLD) MRI scanning, which evaluates deoxyhemoglobin concentration in the kidney, indexed as R2* [17]. Multidetector computed-tomography (MDCT) scanning was used to study single-kidney structure, function, and perfusion. Renal blood flow (RBF) and glomerular filtration rate (GFR) were indexed for body weight. Two days after the completion of *in vivo* studies, pigs were euthanized (pentobarbital sodium, 100 mg/kg IV, Sleepaway®, Fort Dodge Laboratories, Ft. Dodge, Iowa), kidneys were dissected, and sections were frozen in liquid nitrogen (and maintained at -80°C), preserved in formalin, or prepared for micro-CT studies.

Systemic measurements

During MDCT studies, an intra-arterial catheter was placed to record blood pressure. Systemic levels of oxidized low-density lipoprotein (oxLDL), tumor necrosis factor-α (TNF-α), and monocyte-chemoattractant-protein (MCP)-1 were measured by Luminex (Millipore, PCYTMAG-23K) [18], and total cholesterol, triglycerides (TG), low-density lipoprotein (LDL), and high-density lipoprotein (HDL) were measured by standard procedures. IR was characterized by the homeostasis model assessment insulin resistance index (fasting plasma glucose × fasting plasma insulin/22.5).

In vitro studies

Tubular injury was assessed in sections stained with Periodic acid-Schiff (PAS) as described [19]. Absence of brush border, dilation, atrophy, cast formation, cell detachment, or thickening of tubular basement membrane were scored from 1 to 5 based on the fraction of tubules injured (0: normal tubules, 1: <10%, 2: 10-25%, 3: 26-50%, 4: 51-75%, 5: >75%). Glomerular score was assessed as percent of sclerotic glomeruli out of 100 counted glomeruli. Renal scarring was assessed by Masson's trichrome staining, expressed as fraction of kidney surface area, as well as by protein expression of plasminogen activator inhibitor (PAI)-1 and transforming growth-factor (TGF)-β (Western

Table 1. Systemic characteristics and renal function in the experimental groups (n=6/group)

	Normal	RAS	ARAS	MetS + RAS
Body weight (kg)	56.2±6.46	44.8±4.92*	43±3.16*	86±10.05*,†,‡
Mean arterial pressure (mmHg)	92.80±6.56	113.44±20.12*	116.47±22.28*	128.2±7.2*
Degree of stenosis (%)	0.00	83.8±9.86*	89.80±10.3*	93.00±7.58*
GFR (ml/min/kg)	1.6±0.2	0.9±0.1*	1.1±0.1*	1.1±0.1*
Renal blood flow (ml/min/kg)	11.0±0.6	6.5±0.6*	7.9±1.2*	6.8±0.2*
Serum creatinine (mg/dl)	1.39±0.23	1.64±0.18	1.81±0.07*	2.11±0.18*,†,‡
Plasma renin activity (ng/ml/h)	0.21±0.05	0.64±0.46	0.38±0.23	0.90±0.52*
Total cholesterol (mg/dl)	82.00±8.46	80.76±7.55	494.8±54.22*,†	349.6±79.78*,†,‡
HDL cholesterol (mg/dl)	48.60±6.07	52.39±6.47	158.80±42.52*,†	127.60±41.48*,†
LDL cholesterol (mg/dl)	31.92±6.02	33.74±6.49	334.40±34.59*,†	355.16±132.85*,†
Triglycerides (mg/dl)	7.40±2.07	8.18±1.73	8.00±3.39	14.20±15.09
Insulin (mU/ml)	0.40±0.12	0.42±.0.08	0.15±0.08*,†	0.70±0.07*,†,‡
HOMA-IR score	0.62±0.04	0.62±0.08	0.88±0.42	1.94±0.11*,†,‡
Glucose (mg/dl)	121.60±34.05	110.40±30.67	137.8±31.2	123.00±23.03
Oxidized LDL (u/L)	10.0±3.1	12.5±1.7	22.4±3.2*	31.5±9.8*,†,‡
MCP-1 (pg/ml)	142.6±37.9	212.2±126.7	268.1±81.1*	844.2±250*,†,‡
Tumor necrosis factor-α (pg/ml)	21.9±3.0	32.7±1.9*	33.8±5.7*	172.9±33.6*,†,‡

RAS, renal artery stenosis; ARAS, atherosclerotic RAS; MetS, metabolic syndrome; GFR, glomerular filtration rate; HDL, high-density lipoprotein; LDL, low-density lipoprotein; HOMA-IR, homeostasis model assessment of insulin resistance; MCP-1, monocyte-chemoattractant-protein 1. *P<0.05 vs. Lean; †P<0.05 vs. RAS; ‡P<0.05 vs. ARAS (ANOVA, unpaired t-tests).

blot). Apoptosis was evaluated by terminal deoxynucleotidyl transferase dUTP nick-end-labeling (TUNEL) and activated caspase-3 staining. Renal hypoxia was evaluated by Western blotting for hypoxia-inducible factor (HIF)-1α, and angiogenic activity by vascular endothelial growth factor (VEGF), its receptor VEGFR2 (FLK-1), and the angiogenesis inhibitor angiostatin. Renal lipid deposition was measured by oil-red-O staining, and oxidative stress by dihydroethidium (DHE) staining (Life Technologies, D11347, 5 μg/ml) and superoxide dismutase (SOD-1) expression (Western). Inflammation in the kidney tissue was evaluated by protein expression of MCP-1 and TNF-α (Western blot), and the metabolic sensor and anti-inflammatory protein sirtuin-1 (SIRT1). For Western blotting, glyceraldehyde 3-phosphate dehydrogenase (GAPDH) was used as loading control.

Micro-CT

We used a micro-CT scanner to assess microvascular density. Briefly, an intravascular contrast agent (Microfil MV122, Flow-Tech) was perfused under physiological pressure through a cannula ligated in the renal artery. Samples were prepared and scanned at 0.5° angular increments and 18 μm resolution, and the spatial density and size of microvessels in the inner and outer renal cortex were calculated using Analyze™ [20]. Microvessels were classified by diameters as small (20-200 μm), medium (201-300 μm), or large (301-500 μm) [21]. The vascular volume fraction of the tissue was measured as the ratio of the sum of all vessels cross-sectional areas to tissue surface area.

Statistical analysis

All statistical analysis was performed using JMP software package version 8.0 (SAS Institute, Cary, NC). The Shapiro-Wilk Test was used to estimate distribution of the data. Results for normally distributed continuous data were expressed as mean ± SEM. Comparisons among groups were performed using ANOVA and unpaired t-tests with Bonferroni correction. Nonparametric tests (Kruskal-Wallis) were used for data not following a Gaussian distribution. When P<0.05, the difference was considered statistically significant.

Results

Systemic characteristics

Systemic characteristics and renal function in the study groups are summarized in **Table 1**.

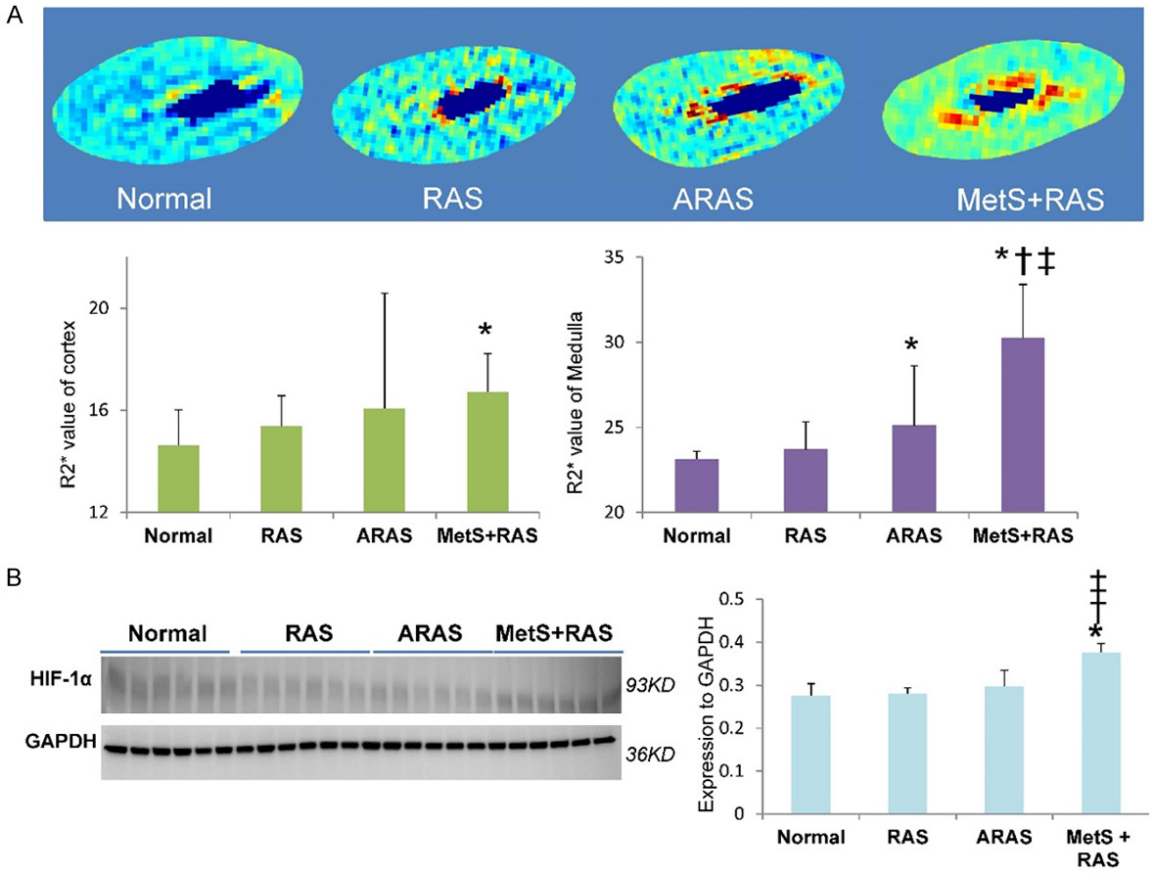

Figure 1. A. Blood oxygenation-level-dependent (BOLD) MRI images of the kidney, and quantification of tissue oxygenation (R2*-index). B. Renal expression of HIF-1α protein was progressively increased in RAS, ARAS and MetS + RAS groups (n=6 each). *P<0.05 vs. Normal; †P<0.05 vs. RAS; ‡P<0.05 vs. ARAS (ANOVA, unpaired t-tests, Kruskal-Wallis).

Body weight in ARAS and RAS groups was similarly lower than that in Normal, but higher in MetS + RAS group. The 3 RAS pigs developed significant stenosis of a similar degree, and blood pressure increased to a comparable level, yet PRA was higher than Normal only in MetS + RAS pigs. Lipid panels were markedly increased in both ARAS and MetS + RAS groups compared to those in Normal and RAS groups. Fasting insulin and HOMA-IR score were elevated only in MetS + RAS group, suggesting a metabolic transition from hyperlipidemia to MetS, whereas glucose levels were not different among the groups. Serum creatinine was higher in ARAS group compared with that in Normal group, and slightly further increased in MetS + RAS group. Stenotic-kidney GFR and RBF were similarly decreased in RAS, ARAS, and MetS + RAS groups compared with those in Normal pigs, indicating development of hemodynamically significant stenoses. Systemic oxLDL levels were elevated in ARAS group and exacerbated in MetS + RAS group. Systemic levels of the pro-inflammatory cytokine TNF-α were progressively increased in RAS and ARAS groups, and further increased in MetS + RAS group, whereas MCP-1 only increased in ARAS group and was further markedly elevated in MetS + RAS group.

MetS + RAS aggravates intrarenal hypoxia

Cortex R2* values were higher only in MetS + RAS than in the Normal group (**Figure 1A**). Medullary R2* values were elevated in both ARAS and MetS + RAS groups compared to Normal group, but MetS + RAS group had significantly higher medullary R2* than ARAS group. Similarly, HIF-1α expression was comparable in the Normal and RAS groups, and progressively up-regulated in ARAS and further increased in MetS + RAS group (**Figure 1B**).

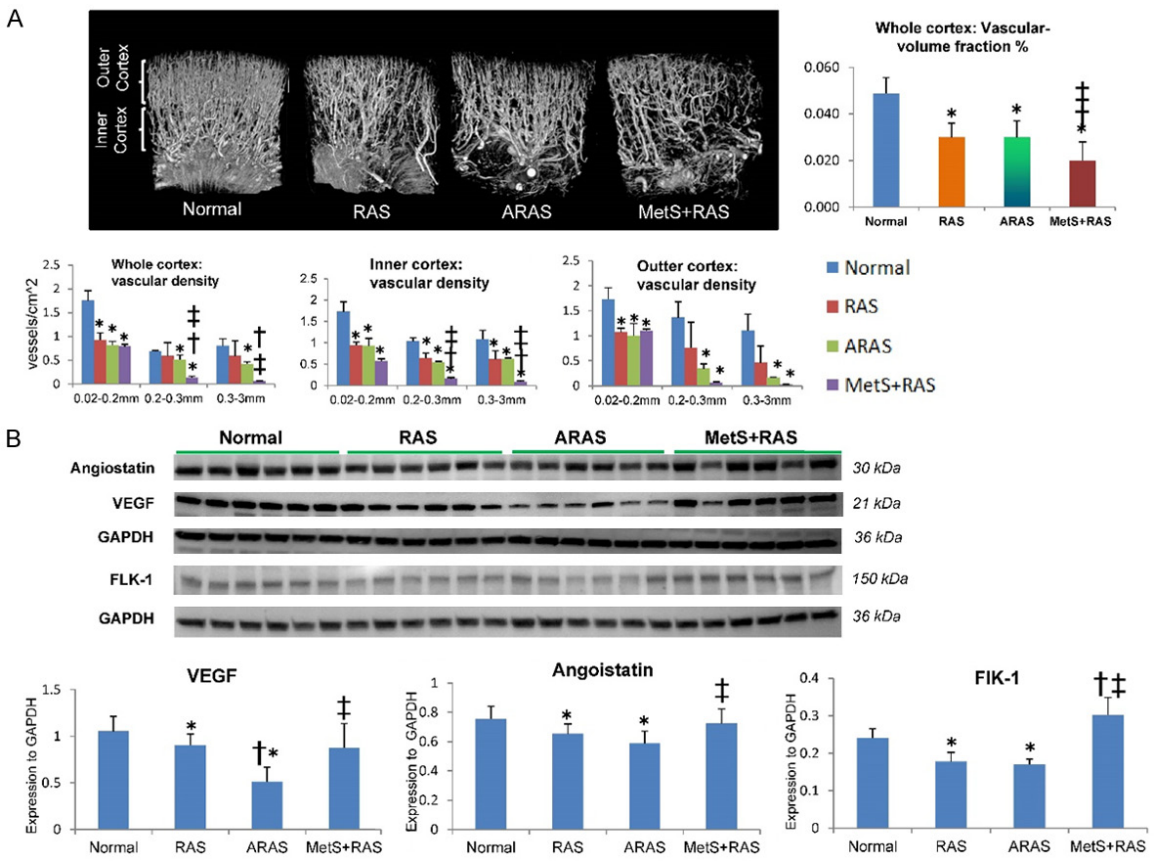

Figure 2. A. Representative 3-D micro-computed tomography images of the pig kidney, and quantification of the spatial density of size-specific microvessels in the whole, inner, and outer cortex. RAS decreased the density of small microvessels (<200 μm) through all cortical regions, and medium-sized microvessels (200-300 μm) in the inner cortex. ARAS decreased the density of all size microvessels throughout the cortex. MetS + RAS further decreased microvessels of all diameter range, and vascular volume fraction, throughout the cortex compared with normal, and in the inner cortex compared also to RAS and ARAS. B. Renal protein expression of VEGF, FLK-1, and angiostatin were progressively decreased in RAS and ARAS, but partly reversed in MetS + RAS (n=6 each group). *P<0.05 vs. Normal; †P<0.05 vs. RAS; ‡P<0.05 vs. ARAS (ANOVA, unpaired t-tests).

MetS + RAS aggravates intrarenal microvascular loss

Compared to Normal pigs, RAS demonstrated a decrease in the density of small-sized microvessels (<200 μm) through the inner, outer, and whole cortex of the stenotic kidney, and medium-sized microvessels (200-300 μm) in inner cortex, while ARAS pigs showed a decrease in the density of all-size microvessels throughout the cortex. However, MetS + RAS pigs showed fewer numbers of microvessels of all diameters throughout the cortex compared to Normal pigs, and in the inner cortex also compared to RAS and ARAS pigs. Of note, MetS + RAS pigs resulted in a lower density of medium-sized and large microvessels compared to ARAS pigs. Congruently, the cortical vascular volume fraction was reduced in RAS and ARAS groups, and further decreased in MetS + RAS group (**Figure 2A**). Conversely, expressions of VEGF and VEGF receptor (FLK-1) were downregulated in RAS and ARAS groups, but not in MetS + RAS group, as was expression of the angiogenesis inhibitor, angiostatin (**Figure 2B**).

MetS + RAS aggravates renal inflammation and oxidative stress

Superoxide anion production in situ as per DHE staining was elevated in RAS pigs compared to Normal pigs, further increased in ARAS pigs, and even further elevated in MetS + RAS pigs (**Figure 3A**). Upregulated SOD-1 expression was only observed in MetS + RAS pigs (**Figure 3B**). Renal expression of MCP-1 was upregulated in

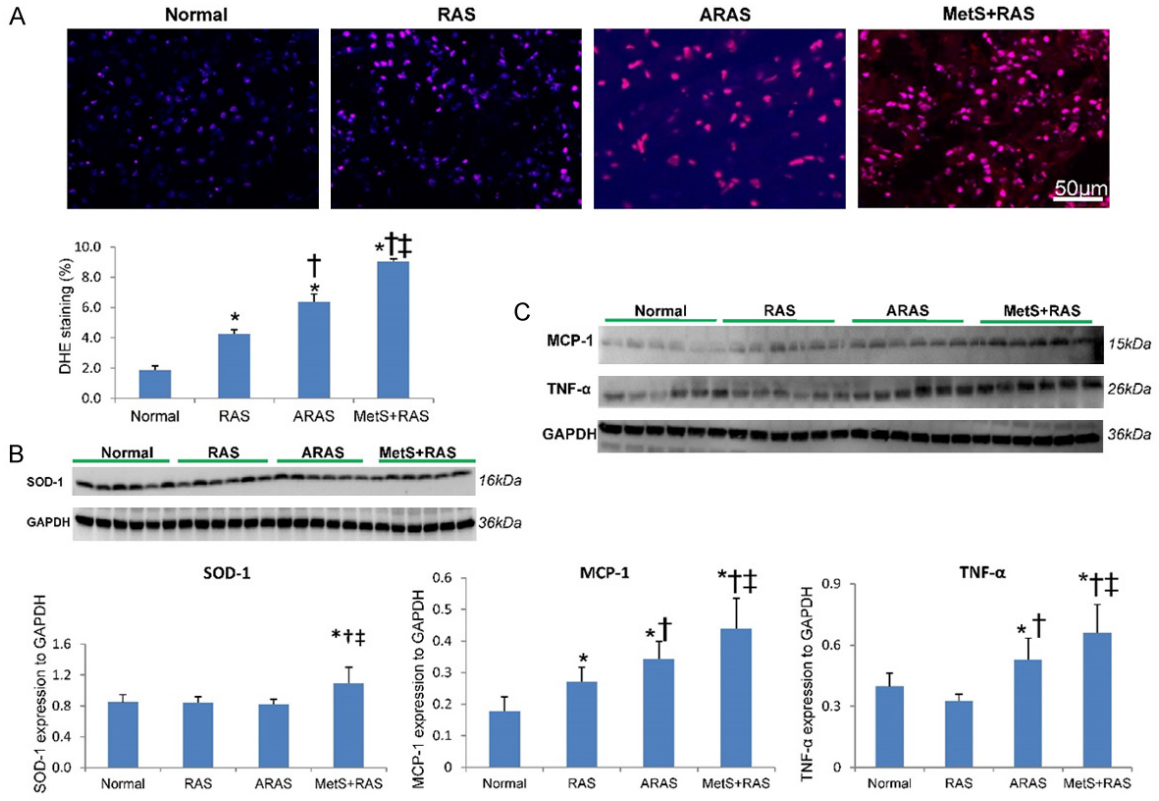

Figure 3. A. Dihydroethidium (DHE) staining and quantifications indicated progressively increased oxidative stress. B. Renal expression and quantification of the anti-oxidant enzyme superoxide dismutase (SOD)-1. SOD-1 expression was markedly upregulated in MetS + RAS. C. Renal expression of the inflammatory markers MCP-1 and TNF-α progressively increased in ARAS and MetS + RAS (n=6 each group). *P<0.05 vs. Normal; †P<0.05 vs. RAS; ‡P<0.05 vs. ARAS (ANOVA, unpaired t-tests).

RAS pigs and was further enhanced in ARAS pigs, yet MetS + RAS pigs had the highest inflammation marker expression. TNF-α had a similar expression pattern, except for RAS pigs which remained unchanged (**Figure 3C**).

MetS + RAS aggravates adiposity and apoptosis

Renal adiposity in RAS kidneys was similar to that of Normal pigs. ARAS goup showed increased lipid deposit only in the medulla, while adiposity in both the cortex and medulla of MetS + RAS group was markedly elevated compared to that of ARAS pigs (**Figure 4A**). Apoptotic activity assessed by TUNEL and caspase-3 staining increased progressively in RAS and ARAS groups and became more pronounced in MetS + RAS group (**Figure 4B**). Renal expression of SIRT1 progressively decreased in RAS and ARAS groups compared with that of Normal group, and MetS + RAS group had comparable SIRT1 expression to ARAS group (**Figure 4C**).

MetS + RAS aggravates tissue injury and fibrosis

PAS staining detected increased tubular injury score in RAS pigs that was further aggravated in ARAS pigs, whereas MetS + RAS pigs showed greater brush-border loss and vacuoles in tubular cells than ARAS pigs (**Figure 5A**). Sporadic focal interstitial fibrosis was observed in RAS kidneys, and became more extensive multifocal in ARAS, while in MetS + RAS group, fibrosis almost doubled compared to that of ARAS group (**Figure 5A**). Similarly, mild glomerulosclerosis was detected in RAS pigs, further exacerbated in ARAS pigs, while MetS + RAS pigs had the highest glomerular score (**Figure 5A**). Expression of TGF-β was progressively increased in RAS, ARAS groups, and further enhanced in MetS + RAS group, whereas the PAI-1 remained unchanged (**Figure 5B**).

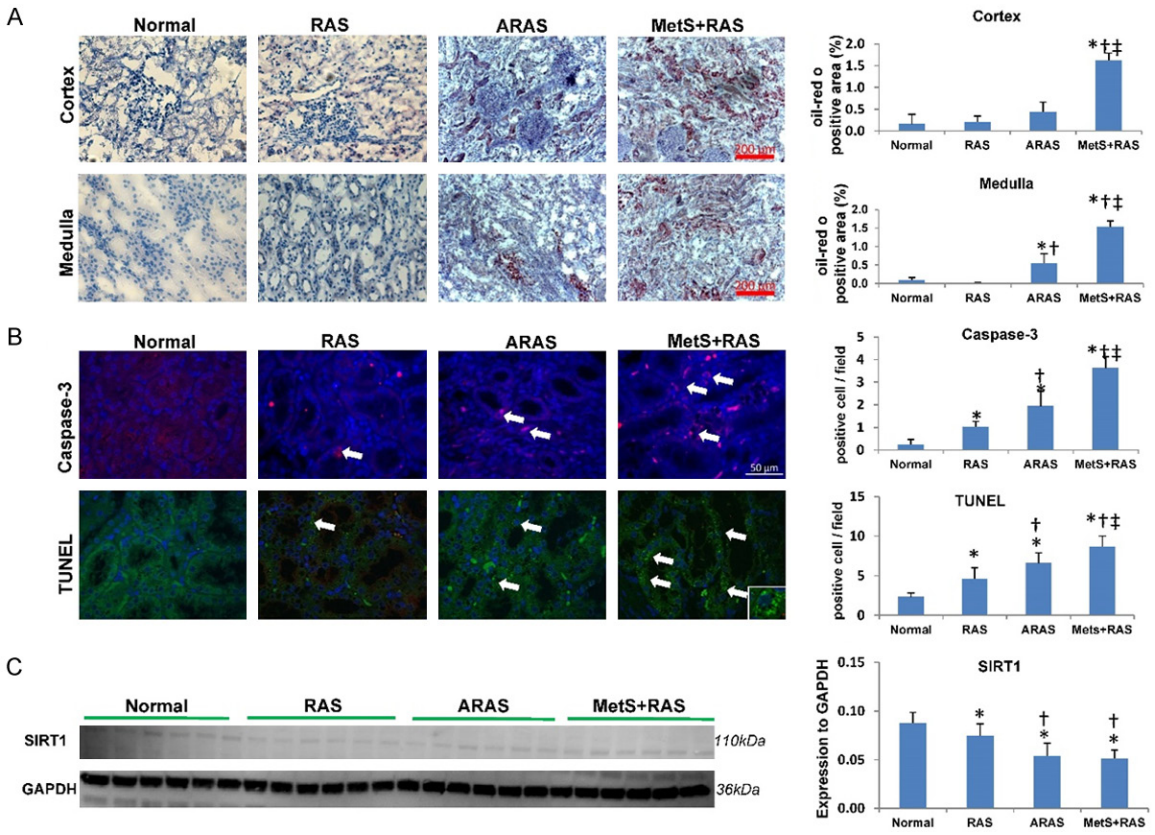

Figure 4. A. Lipid deposits in kidney tissue, indicating significant adiposity increments in the MetS + RAS cortex and medulla; ARAS increased adiposity only in the medulla. B. TUNEL and caspase-3 staining and quantification, indicating a progressively increased kidney apoptosis. C. Renal expression and quantification of SIRT1, showing a progressively decreased SIRT1 expression in RAS and ARAS, whereas MetS + RAS had expression of SIRT1 comparable to ARAS. (n=6 each group). *P<0.05 vs. Normal; †P<0.05 vs. RAS; ‡P<0.05 vs. ARAS (ANOVA, unpaired t-tests).

Discussion

The current study demonstrates that beyond hyperlipidemia alone, development of obesity and IR is associated with magnified systemic inflammation, renal inflammation, and oxidative stress. Obesity and IR also aggravate renal tissue hypoxia, vascular loss, fibrosis, and tubular atrophy, despite preserved renal perfusion and function. These observations suggest that this is in the early phase of the disease. MetS directly exacerbates kidney tissue injury distal to the stenosis and reinforce the importance of abolishing obesity and IR in subjects with renovascular disease.

RAS accounts for a clinical condition, particularly prevalent among the elderly population, which is associated with hypertension, renal injury, and cardiovascular complications [1], and often caused by atherosclerosis [3]. While endovascular therapy for symptomatic RAS might be effective in well-selected patients [22], it does not confer a meaningful benefit in the majority of patients with ARAS when added to comprehensive medical therapy [23]. Superimposition of additional metabolic derangements associated with MetS further undermines the beneficial effect of endovascular intervention in patients with ARAS [4]. These observations imply that mechanisms beyond the main vessel stenosis mediate the direct deleterious effect of MetS on the kidneys to augment damage. Indeed, lifestyle behaviors are potentially modifiable risk factors for people with kidney disease [24]. Our previous studies have suggested that atherosclerosis and hypoperfusion increase renal oxidative stress and inflammation, thereby aggravating renal injury [11, 25]. However, how the development of obesity and IR in MetS interacts with RAS remains unknown. This study extended our pre-

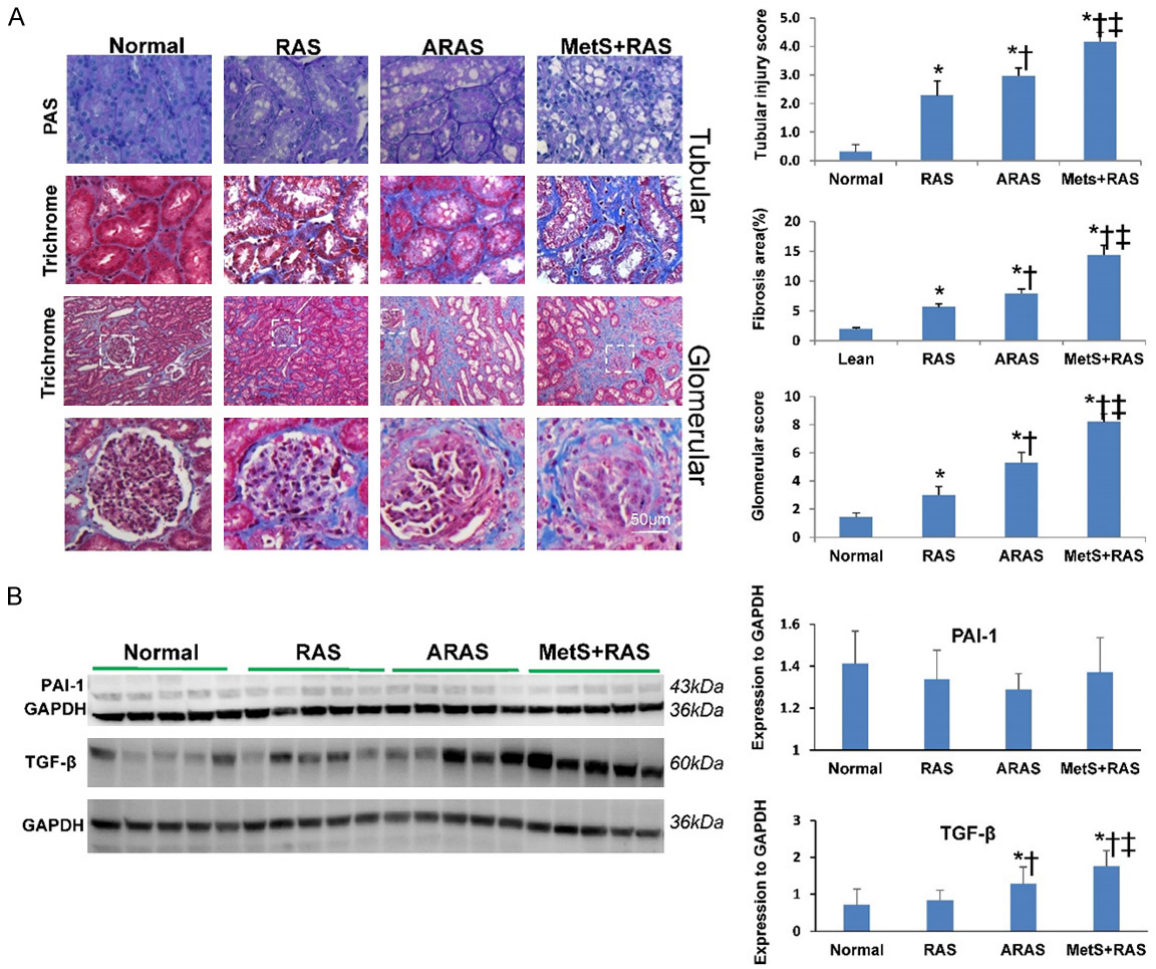

Figure 5. A. PAS and trichrome staining and quantification, indicating progressive kidney tissue injury and fibrosis in the experimental groups. B. Renal expression of the fibrosis markers TGF-β and PAI-1, demonstrating a progressive upregulation of TGF-β in ARAS and MetS + RAS, which was unchanged in RAS. However, there is no significant change of PAI-1 expression increased in RAS, ARAS, and MetS + RAS vs. Normal (n=6 each group). *P<0.05 vs. Normal; †P<0.05 vs. RAS; ‡P<0.05 vs. ARAS (ANOVA, unpaired t-tests, Kruskal-Wallis).

vious findings by showing that the cluster of risk factors represented by MetS magnifies stenotic-kidney microvascular loss and tissue injury beyond the isolated hyperlipidemia observed in ARAS. This might be secondary to multifactorial MetS-associated factors in our study.

In the present study, both the ARAS and MetS + RAS groups were fed with a high-fat diet, but MetS pigs were additionally fed with a high-carbohydrate diet containing 20% fructose. Fructose is involved in the progression to MetS in humans, with increased postprandial plasma lipids [26] and hepatic IR [27], and fructose feeding causes hypertension, hyperinsulinemia [28], dyslipidemia and IR [29]. Dietary fructose induces inflammation, including activation of TNF-α, c-Jun amino-terminal kinase [30], and signal-transducer and activator of transcription-3, which may be responsible for the progression to MetS. In addition, a high-fructose diet increases abundance of the oxidative radical hydrogen peroxide [31], which in turn contributes to development of obesity and IR [32].

Importantly, IR is considered a critical factor linking visceral adiposity to chronic kidney injury. Our previous study has demonstrated that increased adiposity in the MetS heart and kidney correlated with impaired glucose tolerance and development of IR [14, 15]. In the present study, despite slightly lower systemic cholesterol levels, we also found markedly increased lipid deposits in MetS + RAS kidneys in both the

cortex and medulla, while ARAS showed only medullary adiposity. The greater renal adiposity in MetS + RAS might be attributable to the fructose content of the diet, which increases substrate for fat storage in visceral fat tissue [33]. Of interest, adiposity is also increased in the obese pig heart [14], and in the ARAS kidney in the present study, although at a lower extent than MetS, indicating that development of IR does not necessitate marked lipid deposits. Conceivably, adiposity might contribute to IR by altering insulin signaling or glucose metabolism in insulin-responsive tissues, altering release of adipokines to inhibit insulin signaling, recruiting inflammatory cells, or releasing inflammatory cytokines that modulate the insulin-signaling pathway in adjacent or distant tissue [34]. TNF-α and MCP-1 have been implicated in the pathogenesis of IR [35], and organ adiposity is closely related to their levels [36, 37]. In line with this notion, the progressive increase in systemic levels of both MCP-1, TNF-α and renal adiposity in our experimental groups supports a link between lipid deposit-induced systemic inflammation and IR development. In addition, oxidative stress is recognized as a key mechanism in IR [38], and visceral adiposity increases oxidative stress in both obesity and MetS [39, 40]. In the present study, we indeed found no change in systemic oxLDL levels in RAS, but markedly increased levels in ARAS, which were exacerbated in MetS + RAS, indicating lipid oxidation. Possibly, inflammation and oxidative stress induced in other tissues by a high-fat/high-carbohydrate diet may contribute to IR development in pigs.

We have previously shown that chronic inflammation plays a vital role in kidney injury in RAS [19] and ARAS [11]. The current study shows that development of obesity and IR induces progressive renal inflammation in MetS + RAS group, which parallels tissue injury. Its intricate link to inflammation implies that IR might contribute to injury in the stenotic kidney as well. An early clinical study has suggested a close link between microalbuminuria and systemic IR [41]. Subsequent findings indicated a strong relationship between CKD and IR independent of type-2 diabetes [42], and IR conveys an increased risk for progression of CKD to end-stage renal disease [43].

We have found that MetS aggravated post-stenotic kidney injury and fibrosis, accompanied by increased expression of TGF-β and PAI-1. TGF-β signaling impairs renal tubule cell integrity leading to atrophy, a hallmark of tubulointerstitial fibrosis, by inducing epithelial apoptosis or autophagy [44]. This is consistent with our observation that the expression of TGF-β parallels the increased number of TUNEL-positive and caspase-3-positive cells. TGF-β also upregulates expression of PAI-1, which might thereby inhibit extracellular matrix degradation [45], although PAI-1 expression was unchanged in our ARAS and MetS + RAS model. Furthermore, a progressively deceased expression of SIRT-1, which protects the kidney by ameliorating apoptosis, oxidative stress, and inflammation [46], might also play a role in the exacerbation of injury induced by obesity and IR. SIRT-1 not only limits expression of pro-inflammatory genes, but constitutes a central metabolic sensor that regulates energy homeostasis in response to nutrient availability, and is thus particularly relevant to superfluous nutrient states.

Development of obesity and IR in our study also aggravated loss of renal microvasculature, particularly in the inner cortex. Remarkably, renal angiogenic signaling (VEGF and FLK-1 expression) was reduced in RAS and ARAS, but not in MetS + RAS. This was consistent with our previous observations that obese and dyslipidemic swine might show proliferation of cardiac and renal microvessels at the early phase [15, 20], which might initially counterweight ischemia-induced microvascular rarefaction. Yet, these dysfunctional microvessels are susceptible for ultimate loss. On the other hand, MetS upregulates expression of angiostatin that might impair angiogenesis in ischemia [47]. Indeed, unlike RAS and ARAS, MetS + RAS failed to down-regulate angiostatin expression, offsetting the effect of hypoxia [48]. Hence, activation of anti-angiogenic mechanism might have aggravated microvascular loss, in addition to increased inflammation and oxidative stress leading to vasoconstriction and vascular remodeling.

Intriguingly, the decreased cortical microvasculature in MetS + RAS did not aggravate suppression of renal hemodynamics and function, likely due to obesity- or IR-induced hyperfiltration, which might initially counterbalance the loss of renal microvasculature [49]. Alas, vasodilation or increased intravascular blood volume in-vivo are difficult to capture ex-vivo with

micro-CT. Of note, serum cholesterol levels were in fact lower in MetS + RAS than ARAS, indicating that rather than cholesterol levels, obesity and IR may drive renal damage. Vascular loss that was exacerbated in the MetS + RAS inner cortex might interfere with oxygen supply to tubular cells and medullary perfusion at times of heightened need. For example, MetS + RAS-induced glomerular hyperfiltration may increase tubular reabsorption and oxygen consumption that insufficient vessel numbers may be incapable of supporting, leading to medullary hypoxia [50]. Therefore, MetS + RAS triggers a vicious circle leading to severe tissue hypoxia.

Limitations

These experiments were performed in a swine model of RAS accompanied by hyperlipidemia and MetS, to recapitulate the interaction between chronic ischemia and dyslipidemia/metabolic components of human renovascular disease. However, the young age of our pigs, short duration of their exposure, moderate elevation in blood pressure, and unchanged glucose levels all limit the applicability of this model to the clinical scenario. Because the focus of our study was on stenotic kidneys, we did not include a group of MetS pigs without RAS. For a similar reason, we cannot differentiate the contribution of specific components of MetS or fructose in the development of RAS. Thus, future studies are needed to examine the interaction between RAS and individual components of MetS and determine the specific role of each in kidney injury.

Conclusion

Inflammation, oxidative stress, microvascular rarefaction, and fibrosis in the post-stenotic kidney in ARAS are aggravated when obesity and IR develop, suggesting that they further perpetuate a vicious circle of potentially irreversible injury. These observations reinforce obesity and IR as risk factors and therapeutic targets in ischemic kidney disease.

Acknowledgements

This research was partly supported by National Institutes of Health grants DK122734, DK-120292, and AG062104. We thank the China Scholarship Council for their support.

Disclosure of conflict of interest

None.

Address correspondence to: Dr. Lilach O Lerman, Division of Nephrology and Hypertension, Mayo Clinic, Rochester, MN 55905, The United States. Tel: 507-266-9376; Fax: 507-266-9316; E-mail: Lerman.Lilach@Mayo.Edu

References

[1] Wu S, Polavarapu N and Stouffer GA. Left ventricular hypertrophy in patients with renal artery stenosis. Am J Med Sci 2006; 332: 334-338.

[2] Ritchie J, Green D, Chrysochou C, Chalmers N, Foley RN and Kalra PA. High-risk clinical presentations in atherosclerotic renovascular disease: prognosis and response to renal artery revascularization. Am J Kidney Dis 2014; 63: 186-197.

[3] Textor SC and Lerman LO. Renovascular hypertension and ischemic nephropathy: state of the art. Am J Hypertens 2010; 23: 1159-1169.

[4] Davies MG, Saad WE, Bismuth J, Naoum JJ, Peden EK and Lumsden AB. Impact of metabolic syndrome on the outcomes of percutaneous renal angioplasty and stenting. J Vasc Surg 2010; 51: 926-932.

[5] Alberti KG, Eckel RH, Grundy SM, Zimmet PZ, Cleeman JI, Donato KA, Fruchart JC, James WP, Loria CM and Smith SC Jr; International Diabetes Federation Task Force on Epidemiology and Prevention; National Heart, Lung, and Blood Institute; American Heart Association; World Heart Federation; International Atherosclerosis Society; International Association for the Study of Obesity. Harmonizing the metabolic syndrome: a joint interim statement of the International Diabetes Federation Task Force on Epidemiology and Prevention; National Heart, Lung, and Blood Institute; American Heart Association; World Heart Federation; International Atherosclerosis Society; and International Association for the Study of Obesity. Circulation 2009; 120: 1640-1645.

[6] Expert Panel on Detection, Evaluation, and Treatment of High Blood Cholesterol in Adults. Executive summary of the third report of The National Cholesterol Education Program (NCEP) Expert Panel on detection, evaluation, and treatment of high blood cholesterol in adults (Adult Treatment Panel III). JAMA 2001; 285: 2486-2497.

[7] Weiss R, Dziura J, Burgert TS, Tamborlane WV, Taksali SE, Yeckel CW, Allen K, Lopes M,

Savoye M, Morrison J, Sherwin RS and Caprio S. Obesity and the metabolic syndrome in children and adolescents. N Engl J Med 2004; 350: 2362-2374.
[8] Lucove J, Vupputuri S, Heiss G, North K and Russell M. Metabolic syndrome and the development of CKD in American Indians: the strong heart study. Am J Kidney Dis 2008; 51: 21-28.
[9] Navaneethan SD, Schold JD, Kirwan JP, Arrigain S, Jolly SE, Poggio ED, Beddhu S and Nally JV Jr. Metabolic syndrome, ESRD, and death in CKD. Clin J Am Soc Nephrol 2013 8: 945-952.
[10] Chen J, Muntner P, Hamm LL, Jones DW, Batuman V, Fonseca V, Whelton PK and He J. The metabolic syndrome and chronic kidney disease in U.S. adults. Ann Intern Med 2004; 140: 167-174.
[11] Sun D, Eirin A, Ebrahimi B, Textor SC, Lerman A and Leiman LO. Early atherosclerosis aggravates renal microvascular loss and fibrosis in swine renal artery stenosis. J Am Soc Hypertens 2016; 10: 325-335.
[12] McKane WR, Stevens AB, Woods R, Andrews WJ, Henry RW and Bell PM. The assessment of hepatic and peripheral insulin sensitivity in hypertriglyceridemia. Metabolism 1990; 39: 1240-1245.
[13] Xu HY, Barnes GT, Yang Q, Tan Q, Yang DS, Chou CJ, Sole J, Nichols A, Ross JS, Tartaglia LA and Chen H. Chronic inflammation in fat plays a crucial role in the development of obesity-related insulin resistance. J Clin Invest 2003; 112: 1821-1830.
[14] Li ZL, Woollard JR, Ebrahimi B, Crane JA, Jordan KL, Lerman A, Wang SM and Lerman LO. Transition from obesity to metabolic syndrome is associated with altered myocardial autophagy and apoptosis. Arterioscler Thromb Vasc Biol 2012 32: 1132-1141.
[15] Li Z, Woollard JR, Wang S, Korsmo MJ, Ebrahimi B, Grande JP, Textor SC, Lerman A and Lerman LO. Increased glomerular filtration rate in early metabolic syndrome is associated with renal adiposity and microvascular proliferation. Am J Physiol Renal Physiol 2011; 301: F1078-F1087.
[16] Chade AR, Zhu X, Mushin OP, Napoli C, Lerman A and Lerman LO. Simvastatin promotes angiogenesis and prevents microvascular remodeling in chronic renal ischemia. FASEB J 2006; 20: 1706-1708.
[17] Warner L, Glockner JF, Woollard J, Textor SC, Romero JC and Lerman LO. Determinations of renal cortical and medullary oxygenation using blood oxygen level-dependent magnetic resonance imaging and selective diuretics. Invest Radiol 2011; 46: 41-47.
[18] Galili O, Versari D, Sattler KJ, Olson ML, Mannheim D, McConnell JP, Chade AR, Lerman LO and Lerman A. Early experimental obesity is associated with coronary endothelial dysfunction and oxidative stress. Am J Physiol Heart Circ Physiol 2007; 292: H904-H911.
[19] Eirin A, Li Z, Zhang X, Krier JD, Woollard JR, Zhu XY, Tang H, Herrmann SM, Lerman A, Textor SC and Lerman LO. A mitochondrial permeability transition pore inhibitor improves renal outcomes after revascularization in experimental atherosclerotic renal artery stenosis. Hypertension 2012; 60: 1242-1249.
[20] Zhu XY, Rodriguez-Porcel M, Bentley MD, Chade AR, Sica V, Napoli C, Caplice N, Ritman EL, Lerman A and Lerman LO. Antioxidant intervention attenuates myocardial neovascularization in hypercholesterolemia. Circulation 2004; 109: 2109-2115.
[21] Eirin A, Ebrahimi B, Zhang X, Zhu XY, Woollard JR, He Q, Textor SC, Lerman A and Lerman LO. Mitochondrial protection restores renal function in swine atherosclerotic renovascular disease. Cardiovasc Res 2014; 103: 461-472.
[22] Davies MG, Saad WA, Bismuth JX, Peden EK, Naoum JJ and Lumsden AB. Outcomes of endoluminal reintervention for restenosis after percutaneous renal angioplasty and stenting. J Vasc Surg 2009; 49: 946-952.
[23] Cooper CJ, Murphy TP, Cutlip DE, Jamerson K, Henrich W, Reid DM, Cohen DJ, Matsumoto AH, Steffes M, Jaff MR, Prince MR, Lewis EF, Tuttle KR, Shapiro JI, Rundback JH, Massaro JM, D'Agostino RB Sr and Dworkin LD; CORAL Investigators. Stenting and medical therapy for atherosclerotic renal-artery stenosis. N Engl J Med 2014; 370: 13-22.
[24] Schrauben SJ, Hsu JY, Amaral S, Anderson AH, Feldman HI and Dember LM. Effect of kidney function on relationships between lifestyle behaviors and mortality or cardiovascular outcomes: a pooled cohort analysis. J Am Soc Nephrol 2021; 32: 663-675.
[25] Chade AR, Rodriguez-Porcel M, Grande JP, Krier JD, Lerman A, Romero JC, Napoli C and Lerman LO. Distinct renal injury in early atherosclerosis and renovascular disease. Circulation 2002; 106: 1165-1171.
[26] Jeppesen J, Chen YD, Zhou MY, Wang T and Reaven GM. Effect of variations in oral fat and carbohydrate load on postprandial lipemia. Am J Clin Nutr 1995; 62: 1201-1205.
[27] Wei Y, Wang D, Topczewski F and Pagliassotti MJ. Fructose-mediated stress signaling in the liver: implications for hepatic insulin resistance. J Nutr Biochem 2007; 18: 1-9.
[28] Hwang IS, Ho H, Hoffman BB and Reaven GM. Fructose-induced insulin resistance and hypertension in rats. Hypertension 1987; 10: 512-516.
[29] Barros CM, Lessa RQ, Grechi MP, Mouco TL, Souza M, Wiernsperger N and Bouskela E. Substitution of drinking water by fructose solu-

tion induces hyperinsulinemia and hyperglycemia in hamsters. Clinics (Sao Paulo) 2007; 62: 327-334.
[30] Rutledge AC and Adeli K. Fructose and the metabolic syndrome: pathophysiology and molecular mechanisms. Nutr Rev 2007; 65: S13-23.
[31] Nyby MD, Abedi K, Smutko V, Eslami P and Tuck ML. Vascular angiotensin type 1 receptor expression is associated with vascular dysfunction, oxidative stress and inflammation in fructose-fed rats. Hypertens Res 2007; 30: 451-457.
[32] Carrier A. Metabolic syndrome and oxidative stress: a complex relationship. Antioxid Redox Signal 2017; 26: 429-431.
[33] DiNicolantonio JJ, Mehta V, Onkaramurthy N and O'Keefe JH. Fructose-induced inflammation and increased cortisol: a new mechanism for how sugar induces visceral adiposity. Prog Cardiovasc Dis 2018; 61: 3-9.
[34] Hocking S, Samocha-Bonet D, Milner KL, Greenfield JR and Chisholm DJ. Adiposity and insulin resistance in humans: the role of the different tissue and cellular lipid depots. Endocr Rev 2013; 34: 463-500.
[35] Kahn SE, Hull RL and Utzschneider KM. Mechanisms linking obesity to insulin resistance and type 2 diabetes. Nature 2006; 444: 840-846.
[36] Tzanavari T, Giannogonas P and Karalis KP. TNF-alpha and obesity. Curr Dir Autoimmun 2010; 11: 145-156.
[37] Takahashi K, Mizuarai S, Araki H, Mashiko S, Ishihara A, Kanatani A, Itadani H and Kotani H. Adiposity elevates plasma MCP-1 levels leading to the increased CD11b-positive monocytes in mice. J Biol Chem 2003; 278: 46654-46660.
[38] Hurrle S and Hsu WH. The etiology of oxidative stress in insulin resistance. Biomed J 2017; 40: 257-262.
[39] Urakawa H, Katsuki A, Sumida Y, Gabazza EC, Murashima S, Morioka K, Maruyama N, Kitagawa N, Tanaka T, Hori Y, Nakatani K, Yano Y and Adachi Y. Oxidative stress is associated with adiposity and insulin resistance in men. J Clin Endocrinol Metab 2003; 88: 4673-4676.
[40] Palmieri VO, Grattagliano I, Portincasa P and Palasciano G. Systemic oxidative alterations are associated with visceral adiposity and liver steatosis in patients with metabolic syndrome. J Nutr 2006; 136: 3022-3026.
[41] Mykkanen L, Zaccaro DJ, Wagenknecht LE, Robbins DC, Gabriel M and Haffner SM. Microalbuminuria is associated with insulin resistance in nondiabetic subjects: the insulin resistance atherosclerosis study. Diabetes 1998; 47: 793-800.
[42] Chen J, Muntner P, Hamm LL, Fonseca V, Batuman V, Whelton PK and He J. Insulin resistance and risk of chronic kidney disease in non-diabetic US adults. J Am Soc Nephrol 2003; 14: 469-477.
[43] Fox CS, Larson MG, Leip EP, Culleton B, Wilson PW and Levy D. Predictors of new-onset kidney disease in a community-based population. JAMA 2004; 291: 844-850.
[44] Gewin L and Zent R. How does TGF-β mediate tubulointerstitial fibrosis? Semin Nephrol 2012; 32: 228-235.
[45] Visse R and Nagase H. Matrix metalloproteinases and tissue inhibitors of metalloproteinases: structure, function, and biochemistry. Circ Res 2003; 92: 827-839.
[46] Hong Q, Zhang L, Das B, Li Z, Liu B, Cai G, Chen X, Chuang PY, He JC and Lee K. Increased podocyte Sirtuin-1 function attenuates diabetic kidney injury. Kidney Int 2018; 93: 1330-1343.
[47] Dodd T, Wiggins L, Hutcheson R, Smith E, Musiyenko A, Hysell B, Russell JC and Rocic P. Impaired coronary collateral growth in the metabolic syndrome is in part mediated by MMP12-dependent production of endostatin and angiostatin. Arterioscler Thromb Vasc Biol 2013; 33: 1339-1349.
[48] Emara M, Obaid L, Johnson S, Bigam DL and Cheung PY. Angiostatins decrease in the kidney of newborn piglets after hypoxia-reoxygenation. Eur J Pharmacol 2010; 644: 203-208.
[49] Zhang X, Li ZL, Woollard JR, Eirin A, Ebrahimi B, Crane JA, Zhu XY, Pawar AS, Krier JD, Jordan KL, Tang H, Textor SC, Lerman A and Lerman LO. Obesity-metabolic derangement preserves hemodynamics but promotes intrarenal adiposity and macrophage infiltration in swine renovascular disease. AM J Physiol Renal 2013; 305: F265-F276.
[50] Gullans SR, Harris SI and Mandel LJ. Glucose-dependent respiration in suspensions of rabbit cortical tubules. J Membr Biol 1984; 78: 257-262.